# Analyst

## Accepted Manuscript


This is an *Accepted Manuscript*, which has been through the RSC Publishing peer review process and has been accepted for publication.

*Accepted Manuscripts* are published online shortly after acceptance, which is prior to technical editing, formatting and proof reading. This free service from RSC Publishing allows authors to make their results available to the community, in citable form, before publication of the edited article. This *Accepted Manuscript* will be replaced by the edited and formatted *Advance Article* as soon as this is available.

To cite this manuscript please use its permanent Digital Object Identifier (DOI®), which is identical for all formats of publication.

More information about *Accepted Manuscripts* can be found in the **Information for Authors**.

Please note that technical editing may introduce minor changes to the text and/or graphics contained in the manuscript submitted by the author(s) which may alter content, and that the standard **Terms & Conditions** and the **ethical guidelines** that apply to the journal are still applicable. In no event shall the RSC be held responsible for any errors or omissions in these *Accepted Manuscript* manuscripts or any consequences arising from the use of any information contained in them.

($K_2S_2O_8$, 0.1 M) aqueous solution was freshly prepared using PBS (pH 8.0, 0.1 M). Double distilled water was used throughout.

### Apparatus

All electrochemical and ECL experiments were carried out in a conventional three-electrode cell with a modified glassy carbon working electrode (GCE, diameter 3 mm), a Pt wire counter electrode and a saturated calomel electrode (SCE) as reference electrode. Cyclic voltammetric experiments were performed with a CHI 760C electrochemical workstation (CHI, USA). The ECL intensities were measured with MPI-ECL Analyzer (Xi'an Remax Electronic High-Tech Ltd). The photomultiplier tube (PMT) was biased at 800 V in the experiments.[17, 18] Morphologies of the C-dots and Ag-C-dots were characterized by transmission electron microscopy (TEM, JEM-2100). UV-vis spectra were recorded on a shimadzu UV-2450 spectrophotometer (Tokyo, Japan). The fluorescence (FL) spectra were performed on a fluoromax-4 fluorescence spectrofluorometer (Horiba, USA).

### Synthesis of C-dots

C-dots with an average size of ~5 nm used in this work were synthesized according to the literature.[15] Briefly, 1.1 g AA was dissolved in 25 mL deionized water and 25 mL ethanol to form a homogeneous solution. Then, 25 mL as-prepared solution was transferred into autoclave and heated at 180 °C for 4.5 h and then cooled to room temperature naturally. The dark brown solution was extracted with dichloromethane. The water phase solution was dialyzed by employing ester dialysis membranes for three days to remove all impurity molecules. At last, the solution was centrifuged at 8,000 rpm for 30 min, a brown yellow C-dots aqueous solution was obtained.

### Preparation of Ag-C-dots composite

C-dots, obtained from the pyrolysis of AA, contained abundant carboxylic moieties which were suitable for metal ion $Ag^+$ bounding by ion exchange or coordination reactions.[19] The procedure of synthesizing Ag-C-dots composite is illustrated as follows: the as-synthesized C-dots (10 mL, 1.8 mg $mL^{-1}$) were mixed with aqueous $AgNO_3$ solution (2.5 mL, 10 mM) for a few minutes, followed by the addition of NaOH solution (50 µL, 1 M). The reaction was conducted under vigorous stirring at 37 °C for 24 h to obtain the Ag-C-dots composite.

### Electrode modification and detection of $S^{2-}$ ion via ECL

The introduction of $S^{2-}$ ions to Ag-C-dots was conducted by adding various concentrations of $S^{2-}$ ions into 100 µL of Ag-C-dots (4 mg $mL^{-1}$) to generate dispersions of the Ag-C-dots-$Ag_2S$ composite by a vortex mixer for a few seconds. The final volume of the mixture was adjusted to 200 µL with double distilled water. A droplet of C-dots, Ag-C-dots or Ag-C-dots-$Ag_2S$ dispersion with the same amount of C-dots was dropped on GCE, respectively, and dried at room temperature to prepare C-dots/GCE, Ag-C-dots/GCE and Ag-C-dots-$Ag_2S$/GCE modified electrodes. The ECL signals of Ag-C-dots-$Ag_2S$/GCE related to the different concentrations of $S^{2-}$ ions were measured. The whole ECL sensing strategy for $S^{2-}$ ions is shown in Scheme 1.

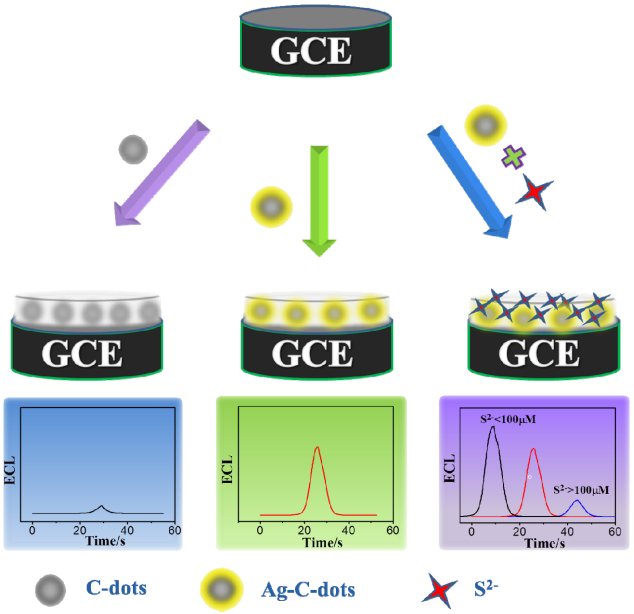


**Scheme 1** Proposed graphic for the detection of $S^{2-}$ ions with Ag-C-dots nanomaterial.

## Results and discussion

### Characterization

UV-Vis and FL spectra were used to characterize the obtained Ag-C-dots, respectively. Fig. 1A shows UV-vis spectra of (a) C-dots (2 mg $mL^{-1}$), (b) Ag-C-dots (2 mg $mL^{-1}$), and (c) Ag-C-dots (2 mg $mL^{-1}$) in the presence of $S^{2-}$ ions (500 µM). Curve a is the typical UV-Vis spectrum of C-dots with the maximum adsorption peak located at ~260 nm.[20] Comparing to C-dots, curve b exhibits another adsorption peak at ~430 nm, which is attributed to the surface plasmon resonance of nanoAg.[16] Fig. 1B is FL spectra of (a) C-dots and (b) Ag-C-dots. With the excitation wavelength of 350 nm, which is consistent with the absorbance peak of C-dots in the wavelength range from 300 to 400 nm (Inset of Fig.1A), the emission wavelength locates at 425 nm, which owes to C-dots fluorescence as reported previously.[15] The obvious quenching effect of transmission metals in FL spectra (Fig. 1B, curve b) indicated the formation of Ag-C-dots nanostructures successfully.[16]

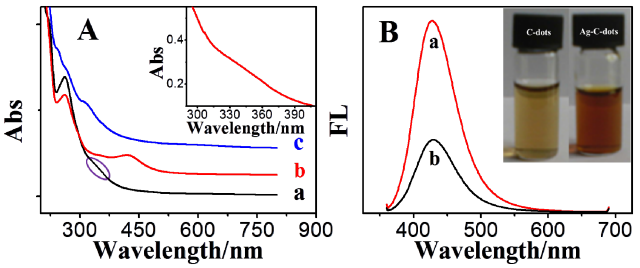


**Fig. 1** (A) UV-vis spectra of (a) C-dots, (b) Ag-C-dots, and (c) Ag-C-dots (2 mg $mL^{-1}$) in the presence of $S^{2-}$ ions (500 µM). Inset: Amplification of UV-vis spectrum of C-dots. (B) FL spectra of (a) C-dots and (b) Ag-C-dots. Inset (from left to right): image of water dispersion of C-dots and Ag-C-dots under visible light.

The as-synthesized Ag-C-dots could be further confirmed by electrochemistry. Comparing with no oxidative-reduction current

Analyst Accepted Manuscript


This journal is © The Royal Society of Chemistry [year]

peaks in the CV of C-dots modified electrode (Fig. 2, curve a), the CV of Ag-C-dots modified electrode in 0.1 M PBS (pH 7) within the potential range of -0.1～0.5 V exhibits a typical pair of oxidative-reduction peaks of nanoAg (Fig. 2, curve b), indicating the existence of nanoAg on Ag-C-dots composite.

To observe the morphologies of the prepared C-dots and Ag-C-dots, TEM was performed. TEM images show that the C-dots are mostly of spherical shape and dispersed rather evenly on the grid surface with the average diameter of ca. 5 nm (Fig. 3, a). The presence of carboxylic groups on the surface of C-dots was supported by the FT-IR spectrum (data not shown). Ag ions are easily bound to the peripheral carboxylic moieties of C-dots by ion exchange or coordination reactions.[19] After reduced by NaOH, the color of the solution gradually changed from light brown to dark red (the inset of Fig. 1B), which demonstrated the formation of Ag nanostructures in the C-dots solution. Meanwhile, it is worth noticing that no nanoAg was observed at the above reaction system in absence of C-dots. Furthermore, it could be observed that C-dots were obviously gathered around nanoAg structure from the TEM image of Ag-C-dots composite (Fig. 3, b), which suggests that C-dots not only take the responsibility to enrich Ag ions to facilitate the reduction reaction, but also act as protective coatings to ensure the production of nanoAg.

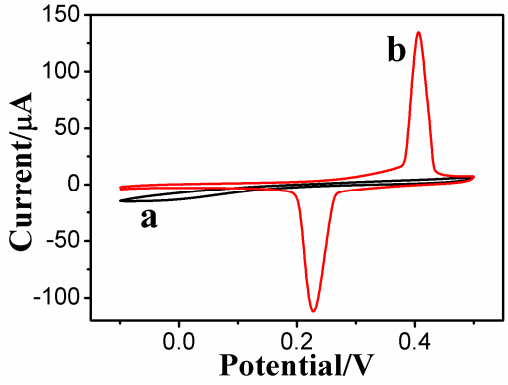


**Fig. 2** CV of C-dots (a) and Ag-C-dots (b) modified electrodes in 0.1M PBS (pH 7.0).

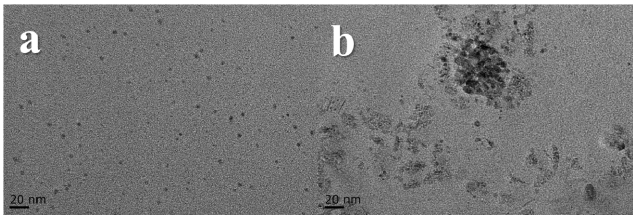


**Fig. 3** TEM images of C-dots (a) and Ag-C-dots (b).

## ECL behaviors of C-dots/GCE and Ag-C-dots/GCE

The electrochemical and ECL behaviors of C-dots/GCE and Ag-C-dots/GCE were investigated by CV. Fig. 4A shows the ECL intensities vs. potential curves for C-dots/GCE and Ag-C-dots/GCE in 0.1 M PBS (pH 8) without and with 0.1 M $K_2S_2O_8$, respectively, at a scan rate of 50 mV $s^{-1}$ within the scan range from 0 to -2.0 V. As expected, no obvious ECL emissions can be observed on both of C-dots/GCE (curve a, Fig. 4A) and Ag-C-dots/GCE (curve b, Fig. 4A) in the absence of $K_2S_2O_8$ as co-reactant. After the addition of 0.1 M $K_2S_2O_8$, an ECL emission of peak potential located at -1.93 V appeared on C-dots/GCE with the onset potential of -1.26 V (curve c, Fig. 4A). Meanwhile, a stronger ECL emission with of potential located at -1.87 V was obtained on Ag-C-dots/GCE with the onset potential of and -0.76 V (curve d, Fig. 4A).

The ECL intensity of Ag-C-dots/GCE was 12.8-fold higher than that of C-dots/GCE with the positive shifts of onset voltages and ECL peak potentials, which are attributed to the better conductivity of nanoAg and more compact film formed by the cross-linking between nanoAg and C-dots. It was reasonable that nanoAg could act as a conducting bridge between C-dots and the electrode to increase the conductivity, thus enhancing the ECL intensity effectively. The ECL emission mechanism was caused by electron transfer annihilation between an anionic quantum dot radical ($R^{\cdot -}$) and the electrogenerated $SO_4^{\cdot -}$.[14] The corresponding ECL processes are described as follows:

$$\text{Ag-C-dots} + ne \rightarrow n\text{Ag-C-dots}^{\cdot -} \quad (1)$$

$$S_2O_8^{2-} + e^- \rightarrow SO_4^{2-} + SO_4^{\cdot -} \quad (2)$$

$$n\text{Ag-C-dots}^{\cdot -} + SO_4^{\cdot -} \rightarrow \text{Ag-C-dots}^* + SO_4^{2-} \quad (3)$$

$$\text{Ag-C-dots}^* \rightarrow \text{Ag-C-dots} + h\nu \quad (4)$$

## The ECL behavior by $S^{2-}$ ions effect

Fig. 4B shows the ECL behaviors of solid-state Ag-C-dots after the introduction of $S^{2-}$ ions. It is very interesting to observe that the ECL intensity increased (curve b) after the introduction of small amount of $S^{2-}$ ions (less than 100 μM), but further addition of $S^{2-}$ ions leads to the ECL intensity decreasing (curve c). The phenomenon is proposed to be related to the synergetic effects of nanoAg functions in Ag-C-dots-$Ag_2S$ system. In fact, nanoAg has two reverse aspects to affect C-dots ECL behaviors. In one aspect, nanoAg can act as a conducting bridge between C-dots and the electrode to increase the conductivity, thus enhancing the ECL intensity effectively. On the other hand, nanoAg can quench the excited state of C-dots by electron transfer, thus decreasing the ECL intensity, which is similar as its FL quenching effect as shown in Fig. 1B.

The surface of the Ag-C-dots possess a small amount of Ag cations/atoms, which have strong and specific interactions with $S^{2-}$ ions.[21] With the addition of $S^{2-}$ ions, $Ag_2S$ should be produced immediately to cover nanoAg. The formation of $Ag_2S$ coating causes the decreasing of conductivity due to the semiconductor of $Ag_2S$. At the same time, the formation of $Ag_2S$ on the surface of the Ag-C-dots could effectively weaken Ag-C-dots bonding to rescue the excited state of the C-dots. To further improve the above suggestions, the optical properties of Ag-C-dots were performed after the introduction of $S^{2-}$ ions. Firstly, UV-Vis spectra were used to monitoring the interaction. It could be observed that the characteristic surface plasmon resonance band of nanoAg centered at ～430 nm was gradually disappeared with the consecutive addition of $S^{2-}$ ions, and that a broad absorbance band for the $Ag_2S$ appeared from the UV-vis spectra (Fig. 4C), confirming the existence of $Ag_2S$ formation.[22] Likewise, the FL intensity (Fig. 4D) gradually increased as the concentration of $S^{2-}$ ions increased, and tended to level off at 100 μM of the $S^{2-}$ ions, indicated that the formation of $Ag_2S$ on the surface of the Ag-C-dots could effectively weaken Ag-C-dots bonding to rescue the FL of the C-dots, and which are consistent with the ECL behavior (Fig. 4B).

Analyst Accepted Manuscript

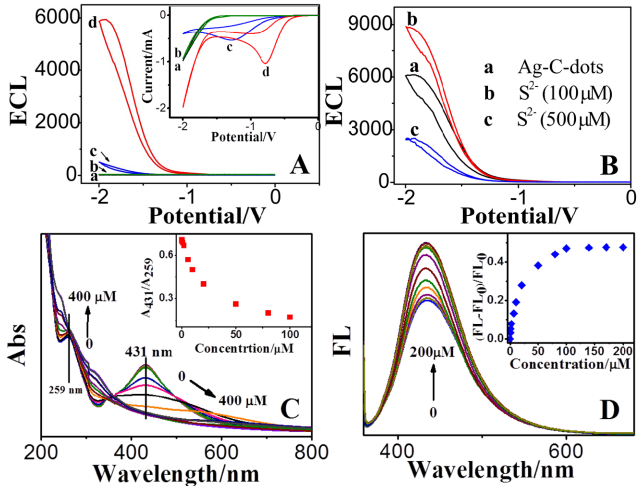


**Fig. 4** (A) ECL vs. potential curves of Ag-C-dots/GCE (a, d) and C-dots/GCE (b, c) in 0.1M PBS (pH 8.0) without (a, b) and with 100 mM $K_2S_2O_8$ (c, d). Inset: the corresponding CV curves, scan rate: 50 mV $s^{-1}$. (B) ECL vs. potential curves of (a) Ag-C-dots, (b) Ag-C-dots with 100 μM $S^{2-}$ and (c) with 500 μM $S^{2-}$ ions on GCE in 0.1 M PBS (pH 8.0) with 100 mM $K_2S_2O_8$. (C) and (D) The UV-vis and FL spectra of Ag-C-dots for the different concentrations of $S^{2-}$ ions.

## The detection of $S^{2-}$ ions by ECL

As discussed above, the detection of $S^{2-}$ ions based on the ECL of Ag-C-dots-$Ag_2S$/GCE includes two linear correlations as the concentration of $S^{2-}$ ions increased. When the concentration of $S^{2-}$ ions below 100 μM, the ECL intensity of the Ag-C-dots gradually increased as the concentration of $S^{2-}$ ions increased, but the concentration of $S^{2-}$ ions above 100 μM, the ECL intensity of the Ag-C-dots gradually decreased as the concentration of $S^{2-}$ increased.

Under the optimized conditions, a semi-logarithmic dependence was obtained between the ratio of the ECL change and $S^{2-}$ ions concentration (Fig. 5A, 5B). The ECL intensity varies linearly with the concentration of $S^{2-}$ ions in two concentration regions, one from 0.05 to 100 μM, another from 100 to 500 μM and the limit of detection (LOD) for $S^{2-}$ ions, at a signal-to-noise ratio of 3, was estimated to be 0.027 μM (~1 ppb), which was much lower than the maximum level of $S^{2-}$ ions in drinking water permitted by the World Health Organization (WHO), namely 15 μM (500 ppb).[23] This approach provided a high sensitivity that was much better than those reported for $S^{2-}$ ions sensors based on optical sensors.[17, 24, 25]

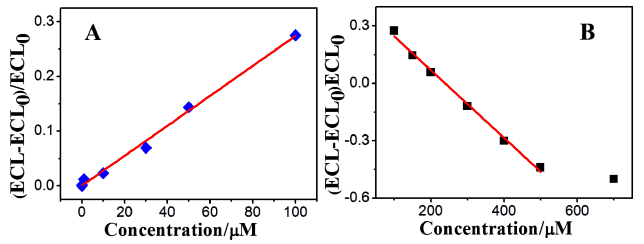


**Fig. 5** (A) and (B) the linear relationship between the degree of ECL intensity change and $S^{2-}$ ions concentration.

Considering the promise of the Ag-C-dots sensor system for application in biological and environmental fields, the selectivity of the sensor for $S^{2-}$ ions was evaluated. The high specificity of $Ag^+ \sim S^{2-}$ interactions[21] provided the excellent selectivity of this method towards detecting $S^{2-}$ ions over other environmentally relevant metal ions. Under the optimal conditions, a series of anions were investigated under similar conditions for the detection of $S^{2-}$ ions (500 μM), such as $SCN^-$, $Ac^-$, $PO_4^{3-}$, $NO_2^-$, $CO_3^{2-}$, $F^-$, $Cl^-$, $I^-$, $ClO_4^-$, $SO_3^{2-}$, and $SO_4^{2-}$ (each 1000 μM), and $Br^-$ was 700 μM. As shown in Fig. 6, $S^{2-}$ ions showed a significant quenching ECL intensity of the Ag-C-dots, while other anions presented only a slight quenching effect.

The significant interference from $I^-$ may be attributed to the formation of the AgI, which its $K_{sp}$ is $8.3 \times 10^{-17}$ $M^2$.[26] To minimize the interference from $I^-$ ions, further investigation demonstrates that $S_2O_8^{2-}$ as a $I^-$ masking agent is able to capture $I^-$ from the AgI precipitation, and $I^-$ reacted with $S_2O_8^{2-}$ to form $I_2$ and $SO_4^{2-}$.[27] As expected, the interference from $I^-$ ions for the Ag-C-dots probe toward $S^{2-}$ ions is negligible in the presence of $S_2O_8^{2-}$ (Fig. 6). The above results validate that the method meets the selectivity requirements of the $S^{2-}$ ions assay in environmental fields.

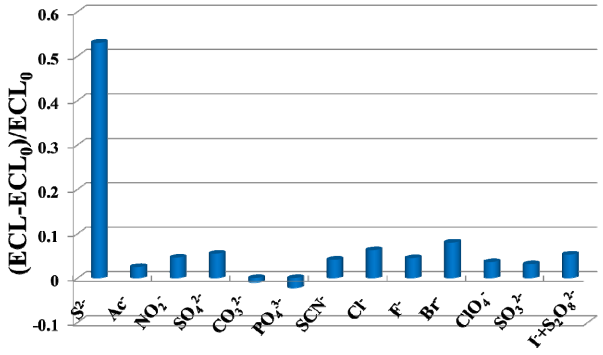


**Fig. 6** Selectivity of the ECL assay for $S^{2-}$ ions over other substances.

## Conclusion

In summary, the Ag-C-dots composite has been prepared using a simple method of direct alkaline reduction in C-dots and $AgNO_3$ mixed solution. The obtained Ag-C-dots nanomaterial exhibit good dispersion and can increased ECL intensity compared with C-dots. The ECL intensity of Ag-C-dots is much changed through the interaction between $S^{2-}$ ions and the Ag atoms/ions on the surface of the Ag-C-dots. Therefore, a sensitive ECL sensing platform to detect $S^{2-}$ ions was fabricated based on the above mechanism. The immobilized technique and the detection methodology is stable, versatile, and rapid, which can be further developed for other environment assays.

## Acknowledgements

This work was supported by the Natural Science Foundation of China (No. 20905011) and the Open Research Fund of State Key Laboratory of Analytical Chemistry for Life Science (SKLACLS1211).

## Notes and references

*Jiangsu Optoelectronic Functional Materials and Engineering Laboratory, School of Chemistry and Chemical Engineering, Southeast*

Analyst Accepted Manuscript



This journal is © The Royal Society of Chemistry [year]

*University, Nanjing 211189, China*
*E-mail: snding@seu.edu.cn (S.N. Ding); Tel/Fax: (+86) 25-52090621;*

1 T. Bagarinao, *Aquat. Toxicol.* 1992, 24, 21-62.
*Methods for the Examination of Water and Wastewater*, American Public Health Association. Washington, D.C., 1971.
4 P.R. Berube, P.D. Parkinson and E. R. Hall, *J. Chromatogr. A*, 1999, 830, 485-489.
5 T. Zhou, N. Wang, C.H. Li, H.Y. Yuan and D. Xiao, *Anal. Chem.*, 2010, 82, 1705-1711.
6 X.F. Yang, L.P. Wang, H. Xu and M.A. Zhao, *Anal. Chim. Acta*, 2009, 631, 91-95.
7 M.I. Prodromidis, P.G. Veltsistas and M.I. Karayannis, *Anal. Chem.*, 2000, 72, 3995-4002.
8 D. Giovanelli, N.S. Lawrence, L. Jiang, T.G.J. Jones and R.G. Compton, *Analyst*, 2003, 128, 173-177.
9 D. Tang and P.H. Santschi, *J. Chromatogr. A*, 2000, 883, 305-309.
10 S.S.M. Hassan, S.A.M. Marzouka and H.E.M. Sayour, *Anal. Chim. Acta*, 2002, 466, 47-55.
11 H.P. Huang, J.J. Li and J.J. Zhu, *Anal. Methods*, 2011, 3, 33-42.
12 Z.F. Ding, B.M. Quinn, S.K. Haram, L.E. Pell, B.A. Korgel and A.J. Bard, *Science*, 2002, 296, 1293-1297.
13 N.S. Baker and A.G. Baker, *Angew. Chem., Int. Ed.*, 2010, 49, 6726-6744.
14 L.Y. Zheng, Y.W. Chi, Y.Q. Dong, J.P. Lin and B.B. Wang, *J. Am. Chem. Soc.*, 2009, 131, 4564-4565.
15 H. Dai, C. Yang, Y. Tong, G. Xu, X. Ma, Y. Lin and G. Chen, *Chem.*
2 X.G. Shen, S. Pardue, K. Fang, S.C. Bir, C.B. Pattillo, G.K. Kolluru and C.G. Kevil, *Biol. Med.*, 2011, 51, S98.
3 M.J. Taras, A.E. Greenberg, R.D. Hoak and M.C. Rand, *In Standard Commun.*, 2012, 48, 3055-3057.
16 L. Wu, J. Wang, J. Ren, W. Li and X. Qu, *Chem. Commun.*, 2013, 49, 5675-5677.
17 S.N. Ding, J.J. Xu, D. Shan, B.H. Gao, H.X. Yang, Y.M. Sun and S. Cosnier, *Electrochem. Commun.*, 2010, 12, 713-716.
18 S.N. Ding, B.H. Gao, D. Shan, Y.M. Sun and S. Cosnier, *Biosens. Bioelectron.*, 2013, 39, 342-345.
19 B. Zhang, C.Y. Liu and Y. Liu, *Eur. J. Inorg. Chem.*, 2010, 28, 4411-4414.
20 L. Tian, D. Ghosh, W. Chen, S. Pradhan, X. Chang and S. Chen, *Chem. Mater.*, 2009, 21, 2803-2809.
21 W.Y. Chen, G.Y. Lan and H.T. Chang, *Anal. Chem.*, 2011, 83, 9450-9455.
22 G. Park, C. Lee, D. Seo and H. Song, *Langmuir*, 2012, 28, 9003-9009.
23 http://www.who.int/water sanitation health/dwq/guidelines/en/.
24 N. Wang, T. Zhou, J. Wang, H. Yuan and D. Xiao, *Analyst*, 2010, 135, 2386-2393.
25 J. Liu, J. Chen, Z. Fang, L. Zeng, *Analyst*, 2012, 137, 5502-5505.
26 K.W. Whitten, R.E. Davis, M.L. Peck and G.G. Stanley, *In Chemistry*, 9th ed., Brooks/Cole-Thompson Learning, Belmont, 2009.
27 D.C. Harris, *Exploring Chemical Analysis*, 3rd ed, W. H.Freeman and Company, New York, 2005.

Analyst Accepted Manuscript